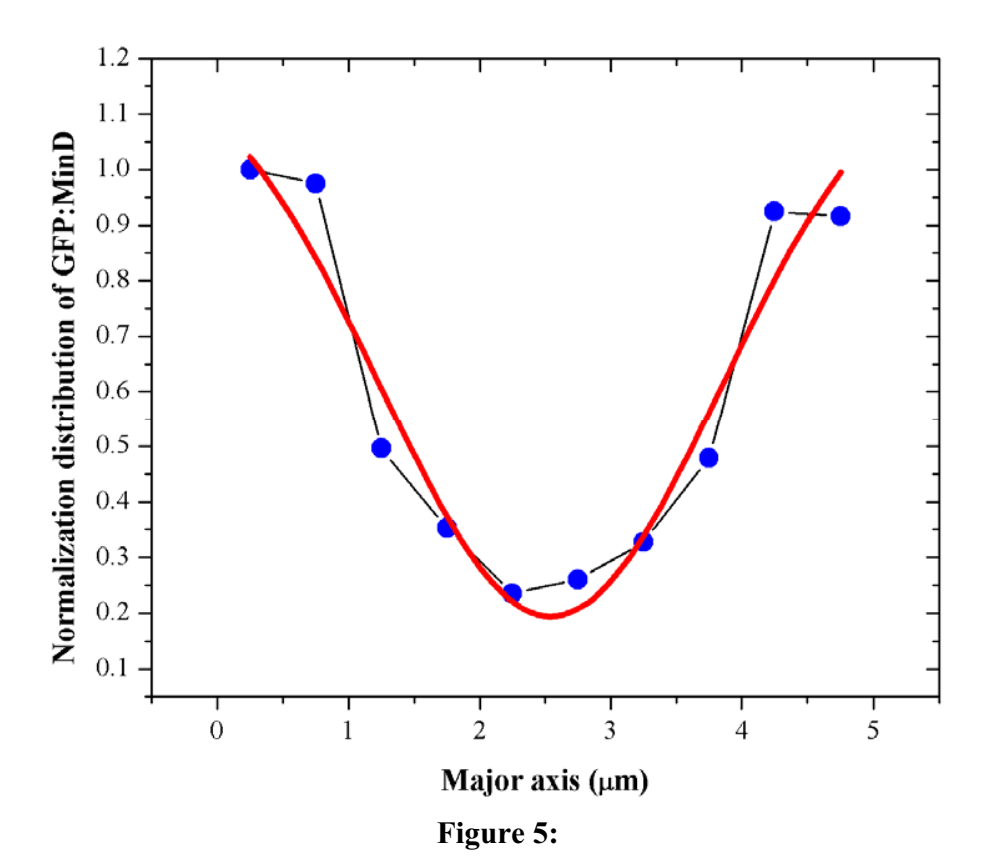


Figure 4:



การจำลองแบบมอนติการ์โลของกระบวนการส่งผ่านและประมวลสัญญาณที่ควบคุมโดยโปรตีนจี MONTE CARLO SIMULATIONS OF SIGNAL TRANSDUCTION MEDIATED BY G-PROTEIN: SPATIAL DISTRIBUTION OF MOLECULES.

<u>อภิวัฒน์ วิศิษฎ์สรศักดิ์</u> วรรณพงษ์ เตรียมโพธิ์ เว

Apiwat Wisitsorasak 1, Wannapong Triampo 1,2

¹Department of Physics, Faculty of Science, ²Capability Building Unit in Nanoscience and Nanotechnology, Faculty of Science, Mahidol University, Bangkok 10400

บทคัดย่อ: คำถามที่สำคัญของกระบวนการส่งผ่านและประมวลสัญญาณคือ ขั้นตอนที่เหมาะสมที่สุด ของการส่งสัญญาณและประมวลสัญญาณคืออะไร จุดมุ่งหมายของงานชิ้นนี้คือ เพื่อจะตรวจสอบ กลไกการส่งผ่านและประมวลสัญญาณที่ควบคุมโดยโปรตีนจี โดยใช้การจำลองแบบมอนติคาร์โล โดยเน้นการศึกษาถึงสารแต่ละชนิดมีการกระจายและจัดตัวเอง เพื่อที่ส่งผ่านและประมวลสัญญาณ สมบูรณ์ได้อย่างไร จากแบบจำลองพบว่า สารบางชนิดมีปริมาณเพิ่มมากขึ้น โดยมีการส่งสัญญาณ ผ่านตัวกลาง ระบบพยายามปรับตัวในภาพรวมให้มีความไร้ระเบียบ ผลการทดลองอธิบายได้ว่า กระบวนการส่งสัญญาณ โมเลกุลซึ่งประกอบด้วยตัวรับสัญญาณและโปรตีนจีพยายามจัดตัวเองให้มี ความไร้ระเบียบแบบเอกรูป

Abstract: A critical question in signal transduction is what is the spatial distribution of involved species to optimize signal transduction processes. The purpose of this work is to investigate kinetics of all considered species including receptors and G-proteins in signal transduction mediated by G-proteins using direct Monte Carlo numerical simulations. The focus is on how each species redistribute or reorganize themselves to optimally achieve this transduction process. It was found that as increasing numbers of particles become large, they are transported into other particles domains and eventually, the system becomes globally completely disordered state. These results may suggest that in signal transduction process, the molecules involved including receptors and G-proteins have tendency to reorganize themselves and become more uniformly disordered.

Introduction: The behavior of a living cell is dictated by its ability to integrate information about its changing environment, a complex biochemical process known as signal transduction. In many systems, receptor/ligand complexes stimulate the activity of G-proteins, which transduce the ligand binding signal across the cell membrane. A critical question in cellular signaling is what is the spatial distribution of involved species to optimize signal transduction processes. The purpose of this work is to investigate kinetics of all considered species including receptors and G-proteins in signal transduction mediated by G-proteins using direct Monte Carlo numerical simulations. The focus is on how each species redistribute or reorganize themselves to optimally achieve this transduction process.

Methodology: We have performed computer to simulate a dynamic stochastic Monte Carlo model of the Ligand-receptor-G-protein system. Dynamics of the system includes diffusion of receptors, receptor-ligand binding/unbinding and their interactions. We divide the cell surface into a grid array. An equal lattice space is about 7 nm. It is defined on a periodic two dimensional rectangular lattices, size of 1000×1000 . Each lattice site is denoted by a pair of integers r = (x, y), and a state index is then assigned to each site of this two-dimensional lattice, taking different values depending on whether the lattice site is vacant, or occupied by either one of six species of particles including: 1) receptors, R, 2) inactive G-protein($\alpha\beta\gamma - GDP$) 3) receptor/ligand complex(C), 4) G-protein components ($\alpha - GDP$), 5) G-protein components $\beta\gamma$, and 6) G-protein components $\alpha - GTP$. Multiple occupancy is forbidden. Initially, receptor

and $\alpha\beta\gamma$ – GDP are placed in the lattice uniform random and periodic boxes (PBC) landscape. After that the system is simulated by the algorithm flow chart (Figure 1).

[1]
$$R \leftrightarrow_{K_r} C$$

[2] $\alpha - GTP \xrightarrow{K_i} \alpha - GDP$
[3] $C + \alpha\beta\gamma - GDP \xrightarrow{K_C} C + \alpha - GTP + \beta\gamma$
[4] $\alpha - GDP + \beta\gamma \xrightarrow{K_\alpha} \alpha\beta\gamma - GDP$
For this simulation, we use total receptor 20000 #/cell, $\alpha\beta\gamma - GDP$ 100000 #/cell Ligand concentration 10^{-6} M, Diffusion coefficient 10^{-11} cm²/s, $K_f = 1 \times 10^6 M^{-1} s^{-1}$, $K_r = 50 s^{-1}$, $K_i = 0.2 s^{-1}$, $K_c / K_i = 250$.

To study the spatial distribution of species, we measure Aggregation Index (AI) (Ref.2) and Shannon Index (SI) (Ref.3) as times progress.

Results, discussion and conclusion: To obtain a visual impression of the signaling process, Fig. 2 shows the evolution of a typical configuration of each species, in a lattice with specified parameters using PBC. The molecules of each type tend to mix with each other and redistribute themselves as time goes on. In Fig. 3, Als are measured, and the results show that Al of all species except $\alpha\beta\gamma - GDP$ increase over time

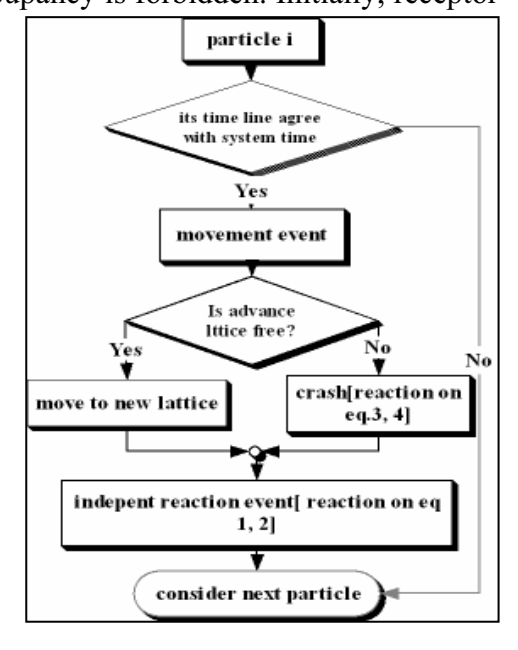


Figure 1. Flow chart of the dynamics

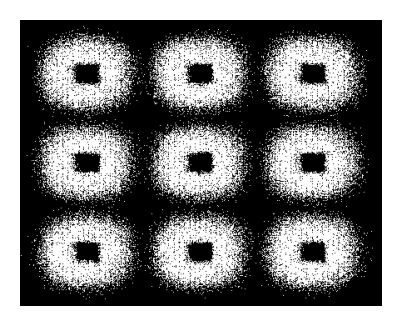


Figure 2. The snapshot of all species. In this picture, we use PBC.

and asymptotically reaches steady state. In Fig. 4, it shows that SI increases as time progresses then reach equilibrium. All these happen may be due to the entropic drive. In conclusion, as increasing numbers of particles become large, they are transported into other particles domains and eventually, the system becomes globally completely disordered state. These results may suggest that in signal transduction process, the molecules involved including receptors and G-proteins have tendency to reorganize themselves and become more uniformly disordered. This may be how nature works!

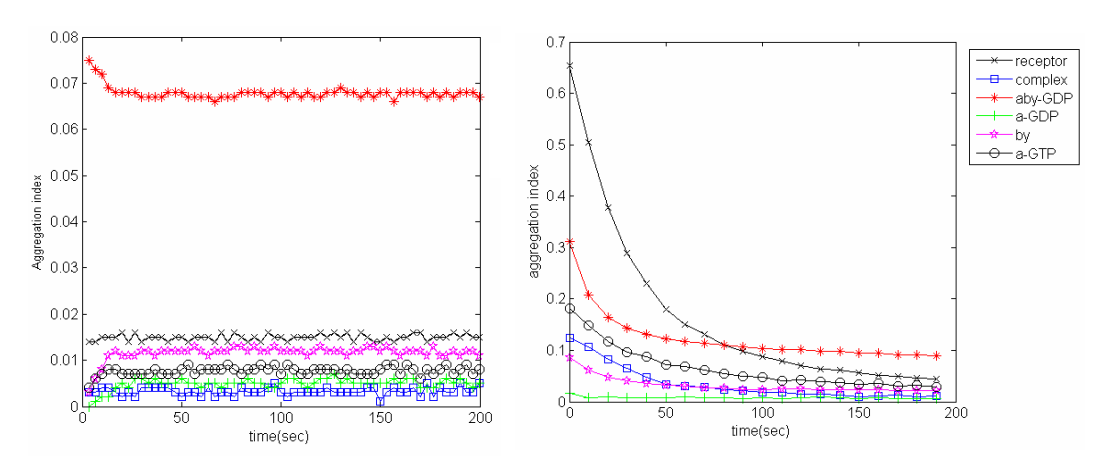


Figure 3. Graphs of AI. (left) uniform condition and (right) PBC

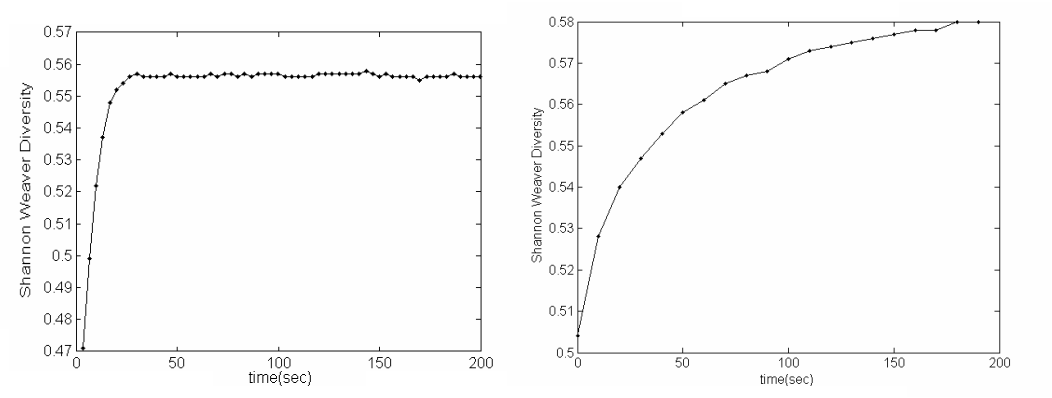


Figure 4. Graph of Shannon Index (left) uniform condition and (right) PBC

Acknowledgements:

This work was supported by by Mahidol University, National Center for Engineering and Biotechnology(BIOTEC), The Thailand Research Fund, and Mahidol University.

References:

- (1) Mahama PA, Linderman JJ (1994) A Monte Carlo study of the dynamics of G-protein activation. Biophys J 67 (3): 1345–1357.
- (2) Hong SH, DeZonia BE and Mladenoff DJ(2000) An aggregation index (AI) to quantify spatial patterns of landscapes. Landscape Ecology 15: 591–601.
- (3) Shannon CE (1948) A mathematical theory of communication. Bell System Tech. J. 27:379–423, 623–656.

Keyword: Signal transduction, G-proteins, Monte Carlo, Aggregation index, Shannon index

ผลกระทบต่อสิ่งแวดล้อมของอนุภาคนาโน : ความเป็นพิษระดับพันธุกรรมของอนุภาคไทเทเนียมได ออกไซด์โดยศึกษาการเกิดไมโครนิวเคลียสในเซลล์ปลาช่อน

ENVIRONMENTAL EFFECTS OF NANOPARTICLES: GENOTOXIC EFFECTS OF TITANIUM DIOXIDE ON INDUCTION OF MICRONUCLEUSE FORMATION IN THE SNAKE HEAD FISH CELL LINE

หฤษฎ์ พิทักษ์จักรพิภพ¹, วรรณพงษ์ เตรียมโพธิ์¹, ลักขณา หิมะคุณ²

<u>Harit Pitakjakpipop</u>¹, Wannapong Triampo¹, Lakana Himakoun²

¹ Department of Physics, Faculty of Science, Mahidol University, Rama 6 Road, Bangkok, Thailand. E-mail: harit chay@yahoo.com

บทคัดย่อ: จากการเพิ่มขึ้นของวัสคุนาโนหรืออนุภาคระดับนาโนในท้องตลาด ในปัจจุบันมีการศึกษา
กวามเป็นพิษและผลทางด้านสิ่งแว้คล้อมยังมีน้อยและผลจากการได้รับอนุภาคเป็นสาเหตุของการป่วย
การศึกษากลายพันธุของเซลล์เป็นการวิเคราะห์ที่ดีเพื่อใช้บอกความเป็นพิษระดับพันธุกรรมเนื่องจาก
มลภาวะของสิ่งแวดล้อม การศึกษาการเกิดไมโครนิวเคลียสในเซลล์ปลาเป็นตัวชี้วัดที่ดีของการ
ตรวจสอบคุณภาพของน้ำจากอุตสาหกรรมและระดับความเป็นพิษระดับพันธุกรรม ในงานวิจัยนี้
ศึกษาการเกิดความผิดปกติในระดับนิวเคลียสในเพาะเลี้ยงเซลล์ปลาช่อนโดยเน้นที่การเปรียบเทียบผล
จากขนาดอนุภาคไทเทเนียมไดออกไซด์ระหว่างอนุภาคระดับนาโนและระดับไมโคร ผลของ
เปรียบเทียบการเกิดไมโครนิวเคลียสของอนุภาคระดับไมโครความเข้มข้นที่ 1, 5, 10 และ 50 ppm กับ
อนุภาคระดับนาโนความเข้มข้น 0.1, 0.5, 1, 5และ 10 ppm ณ ที่เวลาทดสอบ 24, 48 และ 72 ชั่วโมง
สามารถสรุปได้ว่าอนุภาคนาโนมีความเป็นพิษมากกว่าโดยดูจากปริมาณการเกิดไมโครนิเคลียส ผล
จากเพิ่มของความเป็นพิษระดับพันธุกรรมแสดงให้เห็นว่าอนุภาคนาโนเป็นอันตรายต่อมนุษย์และ
สิ่งแวดล้อมโดยที่ขึ้นอยู่กับเวลาที่ทดสอบและปริมาณเป็นสำคัญ เพื่อให้มีความชัดเจนและสมบูรณ์
ต้องศึกษาผลของไทเทเบียมไดออกใชด์เพิ่มในเชิงเวลาที่ทดสอบและปริมาฉอามแข้นข้นต่อไป

Abstract: With the rising of nanomaterials or nanoparticles (NP) in commercial, to date few studies have investigated the toxicological and environmental effects of NP. Exposure to nanoparticle substances can be an important risk factor for human health. Mutagenicity tests represent a good method for genotoxic effect evaluation of environmental pollutants. Several studies have shown that fish micronuclei(MN) tests are sensitive enough to detect genotoxic agents in industrial water, In this work, we have measured MN and monitored nuclear abnormalities in the snake fish cells, with the aim to contribute to the comparative investigation of effects of TiO₂ nanoparticles(TiO₂-NP) and TiO₂ microparticles(TiO₂-MP). The differential sensitivity of fish cells to TiO₂-MP and TiO₂-NP was evaluated by exposing individuals of both species to different doses 1, 5, 10 and 50 for TiO₂-MP and 0.1, 0.5, 1, 5 and 10 for TiO₂-NP. The treatments are monitored over the period of 24, 48 and 72hr. We concluded that TiO₂-NP is more toxic to nuclear material, as it induced higher numbers

Department of Pathobiology, Faculty of Science, Mahidol University, Rama 6 Road, Bangkok,

of micronuclei. The data on increasing of genotoxicity in fish cells indicates a hazard of NP to environments and humans. The doses and the exposure period are important parameters. However, further studies with TiO₂ must be carried out using such as different dose and/or exposure period if we are to reach a better understanding.

Introduction: With the increase of nanomaterials or nanoparticle industries, the central question is whether the unknown risks of NP particularly environmental impact, outweigh the society. Exposure to nanoparticle substances can be an important risk factor for human health. Mutagenicity tests represent a good method for genotoxic effect evaluation of environmental pollutants. In this studies, we have investigate the effects of TiO₂-NP by measuring MN and monitored nuclear abnormalities in the snake head fish cells, with the aim to contribute to the comparative investigation of effects of TiO₂ nanoparticles(TiO₂-NP) and TiO₂ microparticles (TiO₂-MP).

Methodology: Treatment; Because of the low solubility of TiO₂ and in water, a stock solution was prepared by dissolving the desired amount in medium. Treatment was given through aqueous medium for both chemicals, NP and MP. Batches of 3x10⁶ cells each were exposed to 4 doses of MP (1, 5, 10 and 50 ppm) and NP (0.1, 0.5, 1, 5 and 10 ppm). Exposure was continued for 72 hr (3 days) and samples were withdrawn at intervals of 24, 36, and 72 hr by taking out 5 ml per duration in each concentration. Harvested SSN-1 cells were incubated trypsin-EDTA, and sediment mixed thoroughly 3 times with cold fixative then centrifuged and dropped onto clean dry slide with air-dried at room temperature then stained with 10% Giemsa in Weise buffer. The micronucleus frequency was expressed as the number of micronucleated cells per 1000 cells scored. MN were scored under microscope at 100x. Statistical analysis; Each data point represent the mean of 1000 nuclei counted from each of five treated separate cultures from on experiment. We carried out the experiments three times with consistent results. The Analysis of variance (ANOVA) test was used to compare the results of MN (Significant different from the negative control group at P-value < 0.05) using the SPSS 10.0 for PC computers.

Results, Discussion and conclusion: TiO₂-MP are well-known photocatalytic agent that could induce photokilling or bactericidal effects under UV exposure by generating radicals. Not much detailed studies about the effects of theses chemicals in the absence of UV on biological systems. Moreover, no information (or very rare) has been available concerning the effects of these chemicals on snake head fish cells. We have studied the effect of TiO₂ by measuring MN and monitoring nuclear abnormalities in the snake head fish cells and only the effects due to particle sizes and doses are taken into account. MN were observed in all the treatment groups including controls. The size and position of MN in the cytoplasm varied slightly from cell to cell; some were found attached to the cell boundary. Altered nuclear morphology and altered cell morphology were observed with both TiO₂-MP and TiO₂-NP (Fig.1). In the TiO₂-MP treated group (Fig.2a), results revealed that chemicals induced MN formation in a statistically NOT significant manner in comparison with controls. In contrast, in the TiO2-NP treated group, test revealed that NP induced MN in a statistically significant manner in comparison with controls. MN frequency registered a steady rise from 0.5 ppm to 10 ppm at the highest exposure period 72 hr as results of increasing in concentration (Fig. 2b). The significant inductions of MN formation were first observed at concentration 0.1ppm. For concentration 5 and 10 ppm, they were significant for 48 hr induction, and at concentration 10 ppm for 72 hr, as well as 10 ppm for 24, 48 and 72 hr.

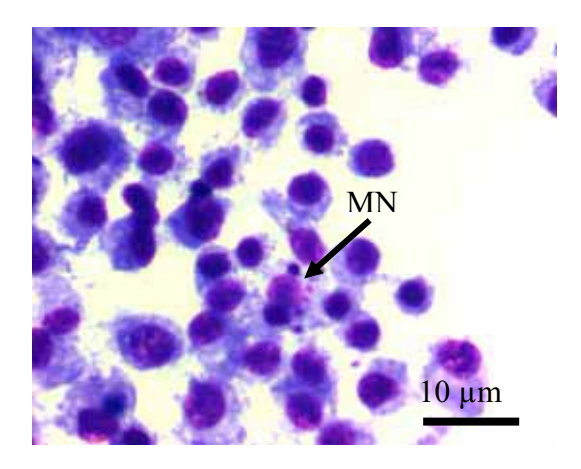


Figure 1: SSN-1 cells exposed to TiO₂-NP (10 ppm, 72 hr), showing induction of MN.

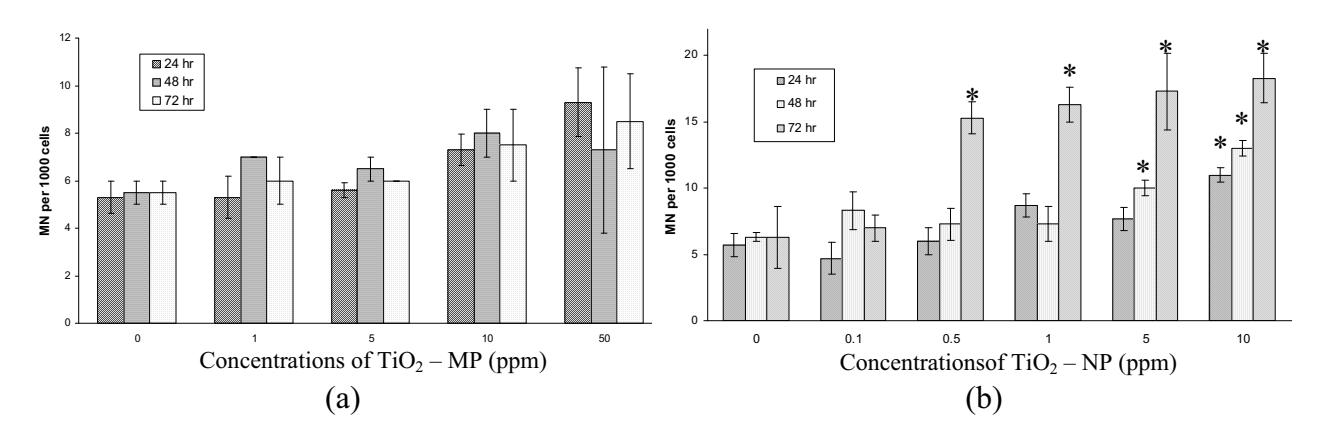


Figure2: Mean values of micronucleus frequencies in SSN-1 cells treatment by TiO₂-MP (a) and TiO₂-NP (b) at different concentrations (ppm) at 24, 48 and 72 hr.

Although our results for MP cases showed small a dose-dependent and exposed time dependent increase in the induction of micronuclei, but it was NOT statistical significant(P<0.05*) in contrast to those treated by NP. TiO₂-NP is more toxic to nuclear material, as it induced higher numbers of micronuclei The data on increasing of genotoxicity in fish cells indicates a hazard of NP to environments and humans.

Acknowledgement: I would like to express my gratitude to Department of Physics and Department of Pathobiology, Faculty of Science, Mahidol University, for the access to all laboratory facilities.

References:

- (1) Kabil Al-Sabti and Chris D. Metcalfe (1995) Mutation Research.343, 121-135.
- (2) Rahman Q., Lohani M., Dopp E., Pemsel H., Jonas L., Weiss D.G., and Schiffmann D.(2002) *Environt Health Perspect.* **110**, 797-800.
- (3) Eva Oberdörster (2004) Environ Health Perspect. 112, 1058-1062.

Keywords: TiO₂-MP, TiO₂-NP, SSN-1, genotoxic, micronuclei

ผลกระทบของอนุภาคนาโนไทเทเนียมใดออกไซด์ร่วมกับแสงอุลตร้าไวโอเลตชนิดเอ ต่อ Letospira interrogans serovar Canicola

Antibacterial effects of TiO₂ nanoparticles combine with UVA on *Letospira interrogans* serovar Canicola

สุดารัตน์ ชาติสุทธิ¹, วรรณพงษ์ เตรียมโพธิ^{1,2}, กัลลยานี ดวงฉวี³, จิระศักดิ์ วงศ์เอกบุตร ¹ Sudarat Chadsuthi ¹, Wannapong Triampo ^{1,2}, Galayanee Doungchawee ³, Jirasak Wong-ekkabut ¹

บทคัดย่อ: จากรายงานพบว่าอนุภาคนาโนของไทเทเนียมไดออกไซด์ (TiO2-NP) ร่วมกับแสงอุลต ร้าไวโอเลตชนิดเอ (UVA) เป็นปฏิกิริยาที่ช่วยเร่งในการฆ่าเชื้อแบคทีเรีย ดังนั้นจึงศึกษาผลกระทบ ที่เกิดจากคุณสมบัติในการยับยั้งการเจริญเติบโตของไทเทเนียมไดออกไซด์อนุภาคนาโนกับเลป โตสไปราซีโรวาร์ Canicola ซึ่งเป็นสาเหตุให้การเกิดโรคฉี่หนู โดยเลี้ยงแบคทีเรียให้ได้ประมาณ 10^8 cells/ml แล้วใส่ TiO_2 -NP 50 µg/ml แล้วนำไปฉายแสง UVA ที่ระยะเวลา 2, 6 และ 24 ชั่วโมง พบว่าที่เวลา 24 ชั่วโมงทั้งที่ใส่และไม่ใส่ TiO_2 -NP มีผลยับยั้งการเจริญเติบโตของ แบคทีเรีย และทดสอบด้วยวิธี immunoblotting พบว่าส่วนประกอบของแอนติเจนน้ำหนัก โมเลกุลที่ 21 และ 48 kDa หายไป ส่วนกลุ่มที่ใส่ TiO_2 -NP เพียงอย่างเดียวให้ผลไม่แตกต่างจาก กลุ่มควบคุม จากผลข้างต้นพอสรุปได้ว่า UVA อาจจะเป็นปัจจัยหลักของการลดการเจริญเติบโต ของแบคทีเรีย ในขณะที่ TiO_2 -NP มีผลกับแบคทีเรียเมื่อได้รับแสงเท่านั้น ควรมีการศึกษาเพิ่มเติม เช่นเปลี่ยนค่าความเข้มข้นและเวลาที่ฉายแสงต่างๆ กัน เพื่อความเข้าใจมากยิ่งขึ้น

Abstract: TiO₂ nanoparticles (TiO₂-NP) combine with Ultraviolet-A (UVA) radiation were recently reported as the photocatalytic disinfection process. Our study is to investigate the antimicrobial effects of TiO₂-NP on L. interrogans serovar Canicola represented as pathogenic leptospires that cause leptospirosis. The bacteria were cultured and treated by TiO2-NP, UVA radiation at variable time duration of 2, 6 and 24 hr with and without TiO_2 -NP at 50 μ g/ $\sim 10^8$ cells-ml. The results show that samples with higher dose UVA (112.3 W-sec/cm²) both with and without TiO₂-NP have higher antimicrobial effects resulting in the decrease in the growth and viability of bacteria when compared with those without UVA exposure. By immunoblotting method, Leptospiral antigen components about 21 and 48 kDa disappear when compared with non-exposed control. Only TiO₂ treatment alone does not significantly give any difference from the control (no treatment) samples. From our preliminary works, it may be concluded that the UVA play a major role on antimicrobial effects while the TiO₂-NP affect bacteria only when photocatalysis is occurred. Further studies with TiO2-NP must be carried out using such as different doses and/or exposure periods if we want to reach a better understanding.

¹Department of Physics, Faculty of Science, Mahidol University, Bangkok 10400, Thailand

²Capability Building Unit in Nanoscience and Nanotechnology, Faculty of Science, Mahidol University, Bangkok 10400, Thailand

³Department of Pathobiology, Faculty of Science, Mahidol University, Bangkok 10400, Thailand

Introduction: Leptospirosis is a zoonotic disease that has become a public health problem throughout the world. It is caused by infection with pathogenic spirochete bacteria of family *Leptospira*ceae and genus *Leptospira* [1]. Proposing, TiO₂-NP that have photocatalytic property [2] as an alternative antibacterial approach could be practical and useful applications. Therefore, understanding more about the effects, side effects and mechanism of how these NP may be used are necessary and important as a first step research concerning this problem. These studies are to investigate the antimicrobial effects of TiO₂-NP on *L. interrogans* serovar Canicola. The bacteria are cultured and treated by TiO₂-NP, UVA radiation with and without TiO₂-NP.

Methodology: In this experiment, bacteria, *L. interrogans* serovar Canicola were cultured until their growth reached a logarithm phase to be used. UVA is generated by 20W T12 fluorescent lamp with continuous emission spectrum 320-400 nm and TiO₂ whose size range 25-70 nm in diameter were purchased from Sigma-Aldrich. TiO₂-NP were then dissolved for the desired amount in medium. The bacteria were cultured and treated by TiO₂-NP at 50 μ g/ \sim 10⁸ cells, UVA radiation at variable time duration of 2, 6 and 24 hr with and without TiO₂-NP, and then sub-culture for 7 days. Conventional scanning electron microscope and spectrophotometer were used to determine the growth, viability and morphology change of the organisms. Protein antigens of experiment characterized using antibody specific to these bacteria by immunoblotting method.

Results: The results in Fig.1 show a decrease of OD (implying the growth) as the exposure time is increased when treated with UVA or UVA+TiO₂. However, OD of those treated by TiO₂ alone does not change from the control group. In Fig.2 the 21 kDa band or LPS (lipopolysacharide) antigens [3] and the 48 kDa identified as a novel OM lipoprotein designated LipL48 [4] present in the unexposed control were disappeared after 24 hr UVA exposure both with and without TiO₂. In Fig.3, from SEM comparison, it is observed that the leptospires from UVA and UVA+TiO2 treated group appeared to be unusual morphology namely more lengthy and longer wavelength.

Discussion and Conclusion: It is well known that UVA can induce cellular and molecular changes such as damage to DNA, protein, and lipids in human and bacterial cells. UVA can induce the formation of oxygen free radicals in the cells. Using combination of UVA and TiO₂ may increase the efficacy of damage or bactericidal effects. These free radicals may cause photoxidation of membrane-bound content and damage the cell membrane. This may result in the lowering of growth and associated denaturation of morphology. However, the finding from pathogenic spirochetes, to the best of our knowledge, is not done yet. From our results, the data show some expected results from e.g., growth and also some unexplainable results such as morphological changes and protein antigens. It may be concluded that the UVA play a major role on antimicrobial effects while the TiO₂-NP affect bacteria only when photocatalysis is occurred. Further studies with NP must be carried out using such as different doses and/or exposure periods if we want to reach a better understanding.

Acknowledgements:

We thank Suchada Gaewdouanglek, Pranom Puchadapirom and Suraphol Kongtim from Department of Pathobiology, Faculty of science, Mahidol University, Bangkok for helpful discussion. This work was supported by The Development and Promotion of Science and Technology Talents Project (DPST), The Thailand Research Fund, The Third World Academy of Sciences (TWAS), and Mahidol University.

References:

- 1. Faine, S., B. Adler, C. Bolin and P. Perolat. (1999) Leptospira and Leptospirosis, Medisci, Melbourne Australia.
- 2. Srinivasan, C. and N. Somasundaram (2003) Bactericidal and detoxification effects of irradiated semiconductor catalyst, TiO₂. Current. Sci. 85, 1431-1438.
- 3. Cullen, P. A., Haake, D. A., Bulach, D. M., Zuerner, R. L. and Adler B. (2003) LipL21 is a novel surface-exposed lipoprotein of pathogenic Leptospira species. Infect. Immun. 71, 2414-2421
- 4. Haake, D. A. and Matsunaga, J. (2002) Characterization of the Leptospiral Outer Membrane and Description of Three Novel Leptospiral Membrane Proteins.Infect. Immun. 70, 4936-4945.

Keyword: Ultraviolet A; TiO₂ nanoparticles; *Leptospira interrogans* serovar Canicola; immunoblot

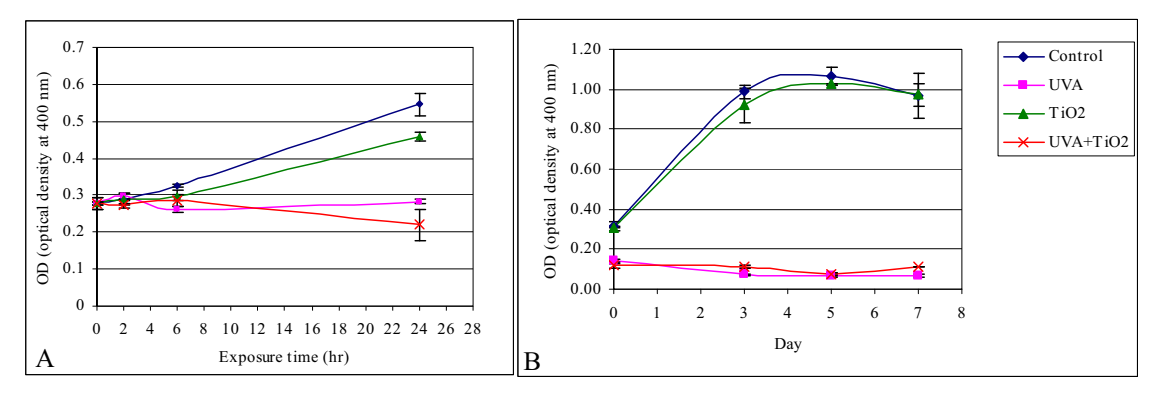


Fig.1 The growth of *L. interrogans* after being exposed (A) and subculture for 7 days (B). It showed relation between optical density at 400 nm for various exposure times at 2, 6, and 24 hr on *L. interrogans* and subculture for 7 days

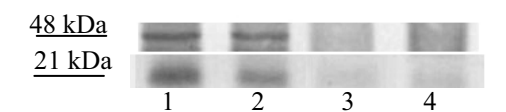


Fig.2 Immunoblot of leptospiral antigen extracted from cells at 7^{th} day of cultivation. Lane 1 is a control. Lane 2 is exposed to TiO_2 at 50 $\mu g/\sim 10^8$ cells-ml. Lane 3 is exposed to UVA. Lane 4 is exposed to UVA with TiO_2 at 50 $\mu g/\sim 10^8$ cells-ml. The 21-kDa and 48-kDa band disappeared at 24 hr of exposure.

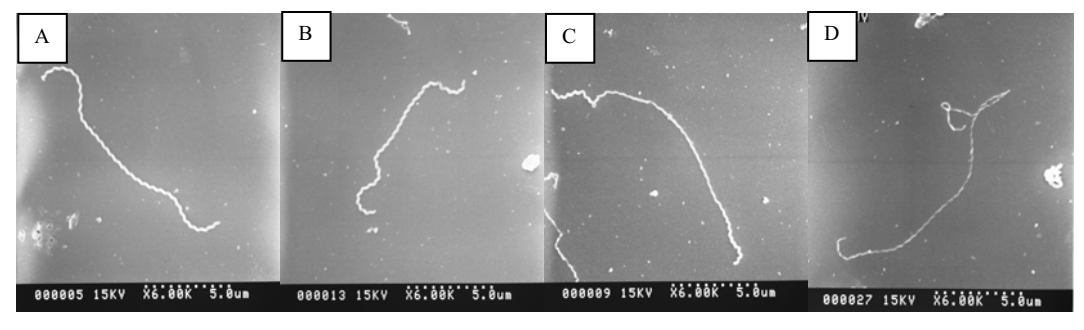
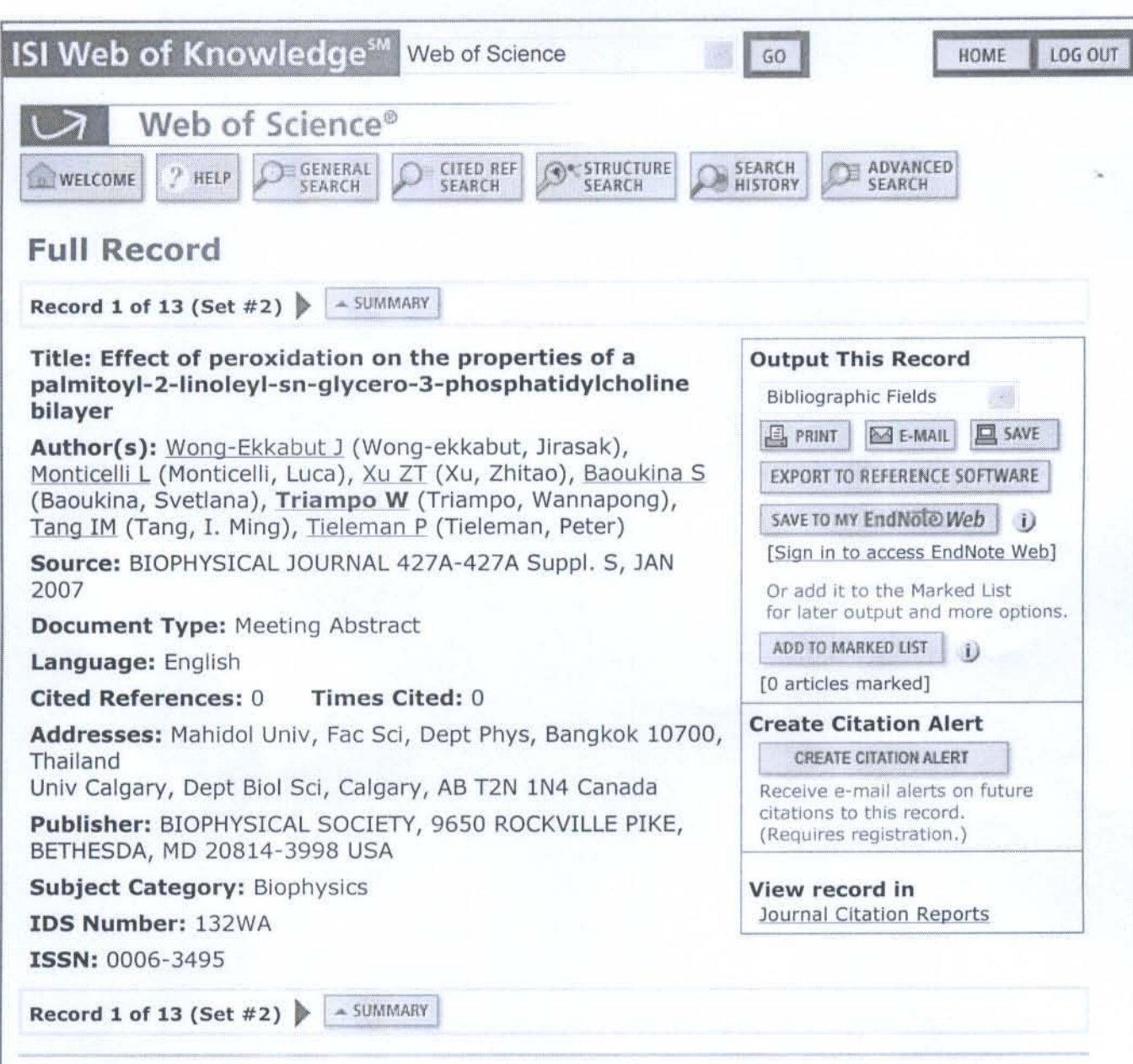


Fig.3 The SEM micrographs of spiral shape. It was taken using scanning electron microscope (Hitachi, Japan) with 15 kV at the magnification 6000x. Control sample unexposed (A) and exposed to TiO_2 at 50 $\mu\text{g}/\sim10^8\text{cells-ml}$ for 24 hr (B) have a consistent wavelength when compared with exposed to UVA with(C) and without (D) TiO_2 at 50 $\mu\text{g}/\sim10^8\text{cells-ml}$ for 24 hr.



Acceptable Use Policy
Copyright © 2007 The Thomson Corporation

C5-page

Biophysical Study of MinD protein oscillation in E. coli

S. Unai, P. Khantang, U. Junthorn, W. Ngamsaad, N. Nattavut, W. Triampo*1, C. Krittanai*2

R&D Group of Biological and Environmental Physics (BIOPHYSICS), Department of Physics, Faculty of Science, Mahidol University, Bangkok, Thailand Institute of Molecular Biology and Genetics, Mahidol University, Bangkok, Thailand

Abstract

The dynamics of MinD is an important factor for accurate positioning of the division septum at the midcell in *E. coli*. The site specificity of *E. coli* cell division, usually at midcell, is regulated by the oscillatory behavior of Min proteins: MinC, MinD and MinE. Previous study of Min protein oscillations focuses on the spatial-temporal pattern formation and the biochemical basis function. However, the experimental data of spatial-temporal pattern formation has not yet quantitatively interpreted. In this work, we use the single particle tracking (SPT) technique which is an unprecedented methodology to explore the dynamics and localizations pattern of GFP:MinD oscillation both in quantitatively and qualitatively. The experimental data are consistent with the previous results and provide some new evidence concerning oscillatory dynamics and localization.

Keyword: MinD protein oscillation, MinCDE system, E. coli, Single Particle Tracking (SPT)

1 INTRODUCTION

Bacterial Cell division is the process by which a cell separates into two after its DNA has been duplicated and distributed into the two regions that will become the future daughter cells. In Escherichia coli (E. coli), for a successful cell division to take place, the cell has to determine the optimal location of the cell separation and the time to start the cell This involves the identification of the cleavage. midpoint of the cell where the septum or cleavage furrow will form. Two processes are known to regulate the placement of the division site: nucleoid occlusion and the action of the Min proteins. Both systems interfere with the formation of a ring of FtsZ protein believed to define the division site. In this research work, we focus on Min proteins oscillation.

In E. coli, the oscillatory dynamics of Min proteins have been played the important role for determining the site of septal placement in cell division, usally at midcell, as the default site for septal placement. The Min proteins consist of MinC, MinD, and MinE expressed from minB operon [3] which facilitates accurate division site at the midcell through the oscillatory cycle from pole to pole [17]. MinC proteins prevent septum formation by inhibiting FtsZ polymerization in vitro [5]. Polymerization of the FtsZ protein into the Z-ring is the first step in septum formation [8, 10]. In vivo, MinC colocalizes and cooscillates with MinD [5, 14] which act together as a negative regulator of Z-ring assembly, and oscillatory dynamics depends on MinE [5, 13, 14]. In vivo, in the absence of MinD, both MinC and MinE remain in the cytoplasm. The minC mutants cells frequently produce minicells because of inappropriate assembly of Z rings

near cell poles [5]. If MinE is absent, MinD will be distributed evenly over the cell membrane [13, 15]. However, the experimental data of spatial-temporal pattern formation has been poorly interpreted for quantitative study [17, 18].

Single Particle Tracking (SPT) is an image processing technique used to follow the high intensity spot of fluorescent particle moving on cell membrane. The data from SPT measurement generally yield a key characteristic of cell membrane. Since it is not only a probe of membrane microstructure but it also has major influence upon reaction kinetics within cell membrane. The SPT technique has been used is a large field of biophysical research. Most of SPT result used to classify the motion of particle and calculate the transport properties; measure the trajectory of individual proteins or lipids in the cell membrane [19], study the dynamics of chromosome [18], mobility Major Histocompatibility Complex analysis of (MHC) Class I molecule on Hela cells [11], study mobility of nuclear trafficking of Viral Genes [1], study the glucose transporter 4 storage vesicles (GSVs) trafficking path way in live cells [2], and bacterial actins motion [9].

In this work, we propose the application of single particle tracking (SPT) technique [12, 19] to explore the dynamics of GFP-MinD protein. The analysis is not only concentrate on the ensemble positions of GFP:MinD, but also on the dynamics and localization via the ensemble positions. Data analysis is performed to provide qualitative and quantitative interpretation on the oscillatory dynamics of MinD.

2 MATERAILS AND METHODS

2.1 Strain and Growth conditions

E. coli RC1/pFX9 [Δ*min*/P_{lac}-*gfp::*Δ*minD* Δ*minE*] was kindly provided by Yu-Ling Shih (Department of Microbiology, University of Connecticut Health Health Center, Farmington)[20]. For examination of MinD labeled with green fluorescent proteins (GFP), cells of RC1/pFX9 were grown in LB medium, 50 μg /ml ampilcillin, 25% of glucose at 37 °C overnight. The OD_{600nm} measurement is approximately 0.4 and before the use of cells, they were diluted with media.

2.2 Image acquisition

For fluorescence image sequence, the Zeiss Axioskop2 of fluorescence microscopy and A-plan, X100, 1.25 oil lenses were used with an InVivo software support in exposure times of 900 ms. A charge-coupled device (CCD) camera (CCD Revolution TM QEI Camera Monochrome) was attached to the video port of microscope to acquire images and movies in 1 frame/second. In our experimental preparation, the 5-7 μ l of sample was dropped in a glass slide coated with 5 μ l of Poly-L-lysine (0.1%) then covered by a cover slip at room temperature (25°C) before examination.

2.3 Image Processing

The Single Particle Tracking (SPT) technique [12, 19] is used to follow the region of interest (ROI) which consists of the highest GFP:MinD concentration signal. We assume highest intensity that is the representation of MinD ensemble in the cell. The gained data in SPT measurement are supported by SpotTracker Java plugin of public domain ImageJ software [22]. The SpotTracker is a robust and fast computational procedure to track fluorescent particles

attached to the molecule of interest in time-lapse microscopy. In this report, the process to be adjacent to the ROI is performed in three steps. The first step is the *E. coli* cell length in the raw fluorescence image sequence was rotated along to the x-axis called major axis shown in **Fig.1** (A). The essential of rotating the *E. coli* cell along to major axis is simple to consider the protein behavior due to the MinD oscillations from pole to pole along the cell length.

In the second step, for acquisition of image sequence as in Fig.1 (A), the fluorescence signal has fade after 4-5 minutes passed; subsequently the final image sequence is noisy. Also for the intensity plot shown in Fig.1 (A'), we see that noisy signal distributes covering all images. This effect causes the accuracy of GFP:MinD ensemble positions collected from SpotTracker. The effect of noise was reduced with Gaussian filter and enhanced to the signal of degraded fluorescence images. This filter was used reducing the effect of noise with 2- pixel radius. If we use a large pixel radius, the positions of ROI are not accurate. The low signal was enhanced by using the rescaling option of SpotTracker plugin as shown in Fig.1 (B), which GFP signal is better than the raw fluorescence images in Fig.1 (A). Similarly for the intensity signal, Fig.1 (B') shows the results of reduced noise that makes the region of high intensity more apparent whereas ROI leads into acquisition of suitable GFP:MinD ensemble positions. The last step is the tracking of ROI with SpotTracker plugin. The tracking results show in Fig.1 (C-C"") which the Red Cross sign denotes for ensemble positions at highest intensity signal (region). After tracking, the positions of ROI are collected in text file ((x,y)) coordinates, for more details of tracking in time algorithm can be found in [18], then the positions of ensemble were analyzed by MATLAB software [mathwork].

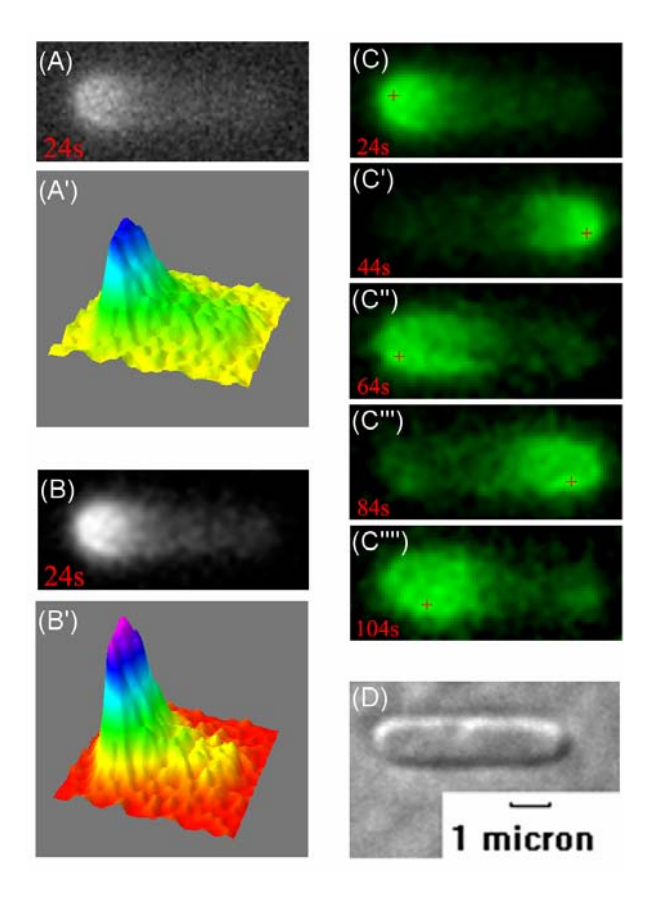


Figure 1: Image processing and SpotTracking results for RC1 *E. coli* cell [min/P_{lac}-gfp::minD minE]. (**A**) shows raw fluorescence image at time 24s. (**A'**) shows intensity plot of fluorescence images corresponding to (**A**). (**B**) fluorescence images of (**A**) after filtering with Gaussian blur and rescaling. (**B'**) shows intensity plot of images (**B**). (**C-C''''**) shows fluorescence images after tracking with SpotTracker at time 24s, 44s, 64s, 84s, and 104s. The positions of ROI are represented in Red Cross sign. (**D**) Shows a DIC image (gray), cell length $\sim 5 \, \mu m$.

3 RESULTS AND DISCUSSIONS

3.1 The single particle tracking (SPT) for GFP:MinD oscillations

The positions at any observable time evolution are collected; we consider those positions along the major (x-axis) and minor axis (y-axis). These separation results display the trajectory of GFP:MinD ensemble in each component as shown the red line on Fig. 2 (B) and (C) respectively.

When Fig. 2 (B) and (C) are compared to Fig. 2 (A), oscillatory dynamics are mostly on the major axis shown in Fig. 2 (D).

In our results, we found that the oscillatory pattern and period (~45 seconds) corresponds to the previous reports [4, 16, 20] as shown in Fig. 2 (A). We see that the pattern of GFP:MinD oscillations, before and after using SPT technique following to Fig. 2 is the same feature. However, the characteristic product of SPT technique is the position which indicates the pattern formation of GFP:MinD ensemble.

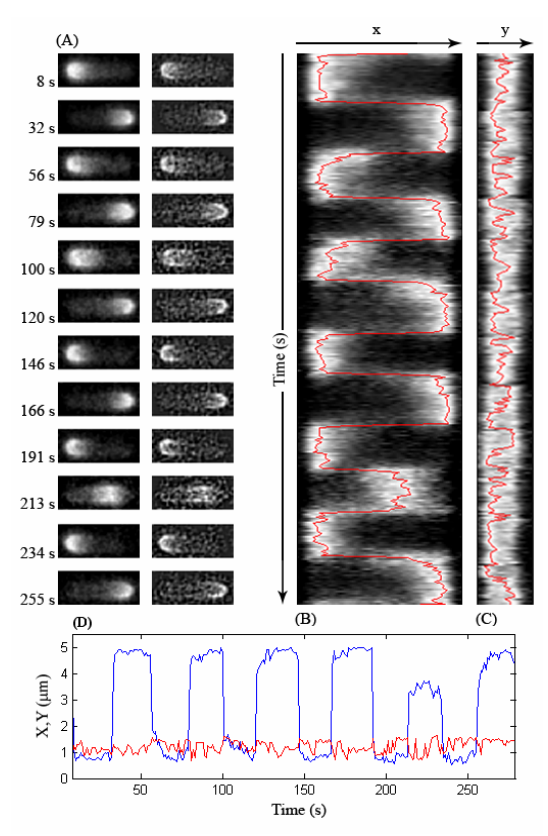


Figure 2: The ensemble GFP:MinD oscillations from pole to pole with the approximately 45 seconds of period with time 8s-279s. **(A)** The pole-to-pole MinD oscillations of 2D image sequence for the rescaled and enhanced signal shown in the left and the right column which each fluorescence image represents the ensemble of GFP:MinD signal locating at polar zones. The time(s) labeled on the left side of column is the first time of GFP:MinD assembles after switching to new pole. **(B)** The results of SPT show the GFP signal time evolution trajectory of MinD oscillations on the x(t)-section. The red line represents the ensemble of GFP:MinD trajectory. **(C)** Spot projection on y(t)-section GFP signal time evolution trajectory of MinD oscillation. **(D)** x-y trajectory time evolution, red line represent trajectory on minor axis, blue line represent trajecxtory on major axis.

3.2 Dynamics of GFP: MinD

The dynamical SPT results of GFP-MinD shown in Fig.3 correspond between the distance and time evolution. The ensemble GFP:MinD protein dynamics can be separated into 2 types; localized dynamics and switching dynamics. The polar zone of *E. coli* performs the localization dynamics (trapping events) because the ensemble GFP-MinD positions have small change in some interval time as shown in Fig.3 (A) (also for Fig.2 (A) and (B) shown in term of GFP-intensity signal or concentration). This situation reflects the velocity at those interval times shown in the time interval between peak to peak in Fig.3 (B). And the velocity at polar zone called the localization velocity.

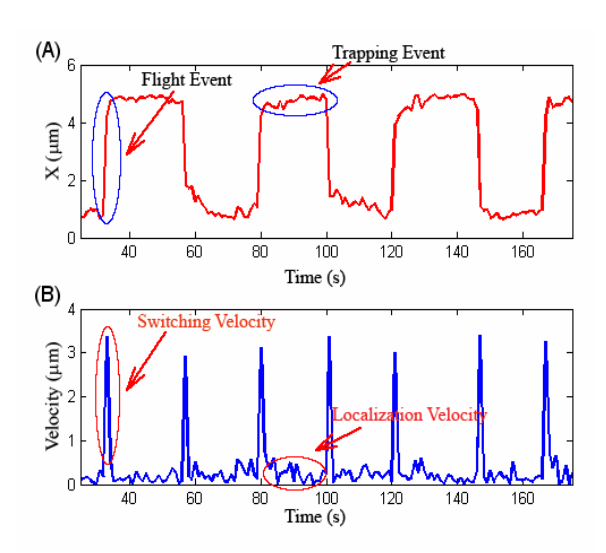


Figure 3: Show trajectory on x-axis and Velocity time evolution 25s-175s interval time. **(A)** Shows Flight events and Trapping events of ensemble GFP:MinD. **(B)** Shows Switching velocity and Localization velocity which correspond to trajectory **(A)**.

When considering the dynamics at polar zones, the trapping events correspond to the polar zone growth by formation of MinD polymerization [7, 23]. The concentration of MinD mostly localizes at poles. Our results describe that the ensemble MinD positions change a little bit, so that velocity time evolution also changes.

For the switching dynamics or flight events, it occurred in some interval time that quickly changing from pole to pole shown in the graph of Fig.3 (A) and (B). This situation is reflected by the switching velocity, which is the velocity of those interval time of velocity time evolution pecks, as shown in the graph Fig.3 (B) and (B'). When compared to the graph of Fig.3 (A), the interval time of switching velocity is the pole-switching position of MinD.

The flight events can be described through Min system dynamics. When MinE activates the ATPase of MinD:ATP polymerized on membrane at the polar zone, MinD:ADP, MinC and MinE released from the membrane into cytoplasm [6, 7, 17, 23]. In the next step, MinD:ADP hydrolyzes a group of phosphate to become MinD:ATP in cytoplasm and diffuses from pole to another pole[5, 13]. While a step of MinD:ATP diffuses to another pole, as a results the flight event and switching velocity occurs.

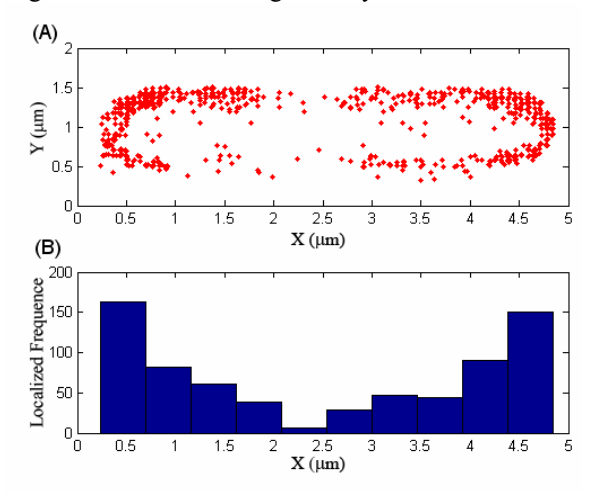


Figure 4: The position scattering and histogram of GFP:MinD localization with 710 seconds. **(A)** is histogram that represent the localized frequency of GFP:MinD along x, y and R respectively. **(B)** Shows the position scattering plot of x-y.

3.3 GFP: MinD Localization.

We have analyzed ensemble GFP:MinD localization though position scattering plot shown in Fig.4(A) and the histogram plot shown in Fig.4(B). This analysis was focused on MinD dynamics at the time average which mean that the observation of MinD dynamics throughout all of observable time. These results perform where MinD proteins mostly localizes. From these analytical results, the histograms

has quantitatively provided us the localization of MinD, while scattering plot of ensemble position has yielded the qualitative information in two dimensional space. Both analytic results reflect the corresponding results which GFP:MinD distribute along the cell length throughout all of observable time mostly concentrate at the polar zones, in the contrary the region near the midcell has the lower concentration as shown in **Fig.4** (A). These results correspond to the previous reports [4, 5, 13, 14] which suggest that the time-averaged concentration of MinD (or division inhibitor) is lowest at midcell.

4 SUMMARY

The goal of this report is to propose the application of SPT for studying MinD dynamics. From our experimental results, position acquisition of ensemble MinD can be characterized and analyzed to achieve dynamic patterns (**Fig.2**, **3**) and localization (**Fig.4**). These results are represented quantitatively and qualitatively in term of dynamics and statics.

Table 1: The physical properties of the ensemble GFP:MinD dynamics.

| Properties | Mean Values | S.D. |
|---|----------------|--------|
| Oscillation Period (s) | 54.63 | 8.55 |
| Switching Velocity (\(\mu m / s \) | 2.95 | 0.32 |
| Localization Velocity (\(\mu m / s \) | 0.2914 | 0.0584 |
| Localization Time (s) | 27.4194 | 4.9666 |

In this study, a measured oscillation period is 54.63±8.55 seconds. Our period measurement is the standard for calculating period of MinD oscillation. This measurement is more accurate than by eye-observed measurement in 2D-image sequence. However, the exact accuracy may not have been demonstrated because of many environmental factors. Recently, a study shows that the period of MinD is dependent on the temperature in which the oscillation period rapidly decreases in proportion to increasing temperature [24].

For the future application, we will investigate the transport properties of the Min protein to be studied through SPT. In mathematical modeling, there are two issues, trapping and flight event, to be investigated in pattern formations.

ACKNOWLEDGMENTS

[24] A. Touhami, et. al. J. Bacteriol. 188 (2006) 7661.

We thank Dr. Narin Nattavut, Asst. Prof. Dr. Wannapong Triampo and Asst. Prof. Dr. Chartchai Krittanai for advice and discuss in this research work. We thank Institute Molecular Biology and Genetics, Mahidol University for *E. coli* cells culture. We thank Yu-Ling Shih (Department of Microbiology, University of Connecticut Health Health Center, Farmington) for strain and plasmid of *E. coli*.

REFERENCES

- [1] H. P. Babcock, et. al. Biophys. J. 87 (2004) 2749.
- [2] C. H. LI, et. al. Cell Research. 14(6) (2004) 480.
- [3] P. A. de Boer, et. Al. Cell 56 (1989) 641.
- [4] C. A. Hale, et. al. EMBO J. 20 (2001) 1563.
- [5] Z. Hu and J. Lutkenhaus, Mol. Microbiol. 34 (1999) 82.
- [6] Z. Hu and J. Lutkenhaus, Mol. Cell 7 (2001) 1337.
- [7] Z. Hu, et. al. Proc. Natl. Acad. Sci. USA 99 (2002) 6761.
- [8] S. S. Justice, et. al. Mol. Microbiol. 37 (2000) 410.
- [9] S. Y. Kim, et. al. Proc. Natl. Acad. Sci. USA 103 (2006) 10929.
- [10] J. Lutkenhaus and S. G. Addinall, Annu Rev Biochem 66(1997) 93.
- [11] R. Patricia, et. al. Biophys. J. 76 (1999) 3331.
- [12] H. Qian, et. al. Single particle tracking. *Biophys. J.* **60:** 910(1991).
- [13] D. M. Raskin, and P. A. de Boer, Proc. Natl. Acad. Sci. USA 96 (1999) 4971.
- [14] D. M. Raskin and P. A. de Boer, J. Bacteriol. 181 (1999) 6419.
- [15] S. L. Rowland, et. al. Membrane redistribution of the Escherichia coli MinD protein induced by MinE. *J. Bacteriol* 182:613-9 (2000).
- [16] L. I. Rothfield, et. al. Cell. 106 (2001)13.
- [17] L. I. Rothfield, et. al.. Nat. Rev. Microbiol. 31 (2005) 959.
- [18] D. Sage, et. al. IEEE Trans Image Process. 14 (2005) 1372.
- [19] M. J. Saxton and K. Jacobson, Annu Rev Biophys Biomol Struct. 26 (1997) 373.
- [20] Y. L. Shih, et. al. Proc. Natl. Acad. Sci. USA 100 (2003) 7865.
- [21] Y. L. Shih and L. I. Rothfield, *MMBR*. 70 (2006) 729.
- [22] SpotTracker: Single particle tracking over noisy images sequence. [Online]. Available:

http://bigwww.epfl.ch/sage/soft/spottracker/ **Web site of ImageJ:** http://rsb.info.nih.gov/ij/

[23] K. Suefuji, Valluzzi, et. al. Proc. Natl. Acad. Sci. USA 99 (2002) 16776.

Effect of TiO₂ Nanoparticles on Pathogenic, Leptospira interrogans

S. Chadsuthi¹, W. Triampo^{1,*}, G. Doungchawee², J. Wong-ekkabut¹, D. Triampo³, and I. M. Tang^{1, 4, 5}

¹R&D Group of Biological and Environmental Physics, Department of Physics,
 Faculty of science, Mahidol University, Bangkok, Thailand.
 ²Department of Pathobiology, Faculty of science, Mahidol University, Bangkok
 ³Department of Chemistry, Faculty of science, Mahidol University, Bangkok
 ⁴Capability Building Unit in Nanoscience and Nanotechnology, Mahidol University
 ⁵Institute of Science and Technology for Research and Development, Mahidol University,
 Nakhonpathom

Abstract

Nanomaterials are wide-range implications in a variety of areas and nanoparticles (NPs) are presently under intensive study for applications. However, increased use of nanometer-sized materials or nanoparticles may cause release of them in the environment. The understanding of effects of nanoparticles on the environment and health are thus crucial but mostly not known.

In this study, we investigate the photocatalytic effects of Titanium dioxide nanoparticles (TiO₂-NPs) undergoing photocatalysis on the pathogenic *Leptospira* serovar Canicola that cause leptospirosis. The leptospires were cultured and treated by TiO₂-NPs, UV-A irradiation with and without TiO₂-NPs groups. The results show that samples with higher dose UV-A both with and without TiO₂-NPs have higher antimicrobial effects resulting in the decrease in the growth and viability of leptospires when compared with those without UV-A exposure. However, the present study is only the first step in assessing the effect of photocatalytic on pathogenic leptospira. Further studies with TiO₂-NPs must be carried out using such as different doses and/or exposure periods if we want to reach a better understanding especially about the mode of action.

Keyword: Titanium dioxide, Leptospira, nanoparticles, UV-A irradiation, photocatalysis, Nanotechnology

Trainian dioxide, Deprospira, nanoparticles, C v 71 interaction, photocentry sis, 1 vanocentrology

1. INTRODUCTION

Titanium dioxide or titania (TiO2) has attracted great attention as an alternative material for water and air purification, photocatalytic sterization in food, and the environmental industry. Recently, the interest has grown in using this process for water disinfection. Although the experimental know-how is extensive, process fundamentals are not yet fully understood. Photocatalysis by TiO₂ could be used as an alternative or a complement to conventional bactericidal activity technologies. It has been intensively conducted on a wide spectrum of organisms including bacteria [1], fungi, algae, virus [2, 3], and cancer cells [4, 5]. When TiO₂ absorbs ultraviolet-A or UV-A light with wavelength less than 385 nm or energy greater than the band gap of TiO₂, it generates electron-hole pairs and migrates to the surface through diffusion and drift [6], in competition with a multitude of trapping and recombination events in the lattice bulk. On the photocatalyst surface, TiO2 particles yield superoxide radicals (O2°-) and hydroxyl radicals (°OH) that can initiate oxidants [7]. The hydroxyl radicals are particularly highly active for both the oxidation of organic substances and the inactivation of bacteria and viruses [8]. Most studies concluded that *OH was the main cause of the bactericidal effect of photocatalysis [9, 10], but the basis for this effect is not well established.

Nanotechnology involves the development and manufacture of materials in the nanometer size range and includes the production and use of nanoparticles (NPs; particles with at least one dimension of less than 100 nm). TiO₂ nanoparticles (TiO₂-NPs) possess interesting optical, dielectric, and photo-catalytic properties. In addition, ultrafine-grained compacts of titania, the so called nanophase, are expected to have high mechanical strength and a low sintering temperature. These nanometer-sized effects are caused by the large surface-to-volume ratio, resulting in more atoms along the grain boundaries than in the bulk material.

Previously, most studies of the effects of TiO₂-NPs on biological systems, with and without UV-A irradiation are mainly focused on *Escherichia coli* [11, 12]. Nevertheless, there have not been any experiments to focus on pathogenic spirochetes,

^{*}Corresponding author. Tel: +662-201-5770; Fax: +662-354-7159; Email: wtriampo@yahoo.com

especially genus *Leptospira*. Leptospira have a typical double membrane structure in common with other spirochetes, and share characteristics of both Gram-positive and Gram-negative bacteria [13]. The periplasmic flagella of leptospira are located between the two outer membranes [14]. Leptospira cause leptospirosis, an acute febrile illness [15, 16]. The illness can range from being a mild flu-like illness to being a severe (often fatal) illness involving renal and/or liver failure and hemorrhage (referred to as Weil's syndrome) [17]. This disease has emerged as an important public health problem worldwide. Mammals such as rats and cattle are commonly involved in the transmission of this disease to humans via direct or indirect exposure through contaminated tissues or urine.

In this work, we have compared the effects of TiO₂-NPs with and without UV-A irradiation on the spirochete bacterial pathogens, namely, *Leptospira interrogans* serovar Canicola. The main purpose of this study is to investigate the effects of exposing on different dosages. The cell growth and viability were determined by UV-VIS spectrophotometry and dark field microscopy. Transmission electron microscopy was used to confirm the surface membrane changes in the different treatment.

2. MATERIALS AND METHODS

2.1 Strain and Culture Condition of Leptospira

Pathogenic Leptospira interrogans serovars Canicola were obtained from the National Leptospirosis Reference Center, National Institute of Health (NIH), Thailand and maintained by weekly subculture at 28-30 °C in liquid DifcoTM Leptospira Medium Base EMJH (Becton, Dickinson and Company; Sparks, MD, USA) [16, 18]. Leptospira samples have an initial optical density (OD) at 400 nm of about 0.15~108 cells/ml as measured by a UV-VIS spectrophotometer.

2.2 UV-A Radiation Source and TiO₂ Nanoparticles

In this experiment, the UV-A radiation is generated by a 20W T12 fluorescent lamp with continuous emission spectrum 320-400 nm and a peak at 365 nm. The UV-B and UV-C radiations are absorbed by the glass tube. The leptospira were exposed to an UV-A radiation of intensity of about 13 W/m².

TiO₂ nanoparticles (TiO₂-NPs) were bought from Sigma-Aldrich (St. Louis, MO), commercial name Titanium (IV) oxide (nanopowder, 99.9 %). These particles a mix of anatase and rutile form. The average particle sized characterized by the XRD technique was

specified as 25-70 nm. The surface area of TiO_2 -NPs is 20-25 m²/g. The characteristics and details of these particles can be obtained from the distributor [19]. For experimental use, TiO_2 -NPs were autoclaved at 121°C and 103 kPa for 15 minutes for sterilization before used.

2.3 Growth, Cell Survival, and Morphology

The three techniques mentioned above were used to monitor the leptospira growth, survival, and morphology.

Quantitative analysis by UV-VIS spectroscopy

The cell density of leptospira were determined by UV-VIS spectrometer (V-530 UV/VIS spectrometer, Jasco Internationl Co.,Ltd.). Solutions of the leptospira were placed into cuvettes made with quartz SUPRASIL (200-2500 nm) with light path 10 mm (type no. 100.600-QG, Hellma Co.) for UV-A exposure and placed into disposable cuvettes for exposed TiO₂-NP with and without UV-A. A single beam spectrometer operating in the range of 200 to 800 nm was used. The optical density or absorbency at 400 nm was taken [20, 21]. All samples were obtained with already used EMJH liquid medium with or without TiO₂-NP as the blank.

Qualitative analysis by dark-field microscopy (DFM)

The growth and viability of the treated leptospira were determined by looking at cell density, mobility [22], and morphology. In DFM, an oblique light beam is cast onto the leptospira (lying on a microscope slide) by the use of a special condenser, when the central illuminating light beam is interrupted. The leptospira can then be seen as silvery threads in a dark background.

Transmission Electron Microscopy (TEM)

In electron microscopic examination, the leptospira were concentrated by centrifugation at 10,000 RPM for 10 min, and prefixed with 1.5% glutaraldehyde containing 0.1 M phosphate buffer, pH 7.2, at 4°C for 2 hr followed by postfix with 1% osmium tetroxide solution containing 0.1 M phosphate buffer at room temperature for 1 hr and subsequent steps as described [23]. The samples were examined under a transmission electron microscope (TECNAI 20).

2.4 Experimental procedure

Leptospira interrogans serovar Canicola were cultured in a EMJH medium until the logarithmic growth phase and then diluted to optical density (OD)

= $0.15 \sim 10^8$ cells/ml to be used. The suspensions of leptospira were treated with TiO₂-NPs at 50 µg/ml group and TiO₂-NPs at 50 µg/ml with and without UV-A irradiation at 13 W/m² for 2, 6, and 24 hrs of exposure time. After exposure, all samples were taken for measurements of their viability and growth using a dark-field microscope and UV-VIS spectrometer. Then, all samples were subcultured for a further 7 days. On 7^{th} day post-treatment, Micrographs were taken using transmission electron microscope. Experiments were repeated at three times under the same conditions with separated occasions.

The statistical analysis was used to analyse the effects of TiO₂-NPs at 0.05 mg/ml, and TiO₂-NPs at 0.05 mg/ml with and without UV-A groups on leptospira. The results show significant differences between groups are defined as those with P-values less than 0.05.

3. RESULTS

3.1Effect on Viability and Growth

Figure 1 aims to quantitatively see how the treatments affect the viability of *Leptospira interrogans* serovar Canicola and the correlation between the viability and treatments. It shows that the OD decreases as the exposure or illumination time is increased when treated by UV-A with and without TiO₂-NPs. However, the OD of those treated by TiO₂-NPs alone does not change from the control group. These results surprisingly show the similarity of the photokilling (by UV-A alone) and photocatlytic killing (UV-A with TiO₂-NPs) which is unexpected as far as the previous results (on other types of microorganisms) are concerned [1, 2, 12, 17, 25-27].

To monitor the long time or accumulated effects of each treatment, each sample was subcultured and cultivated for 7 days after the treatment. The growth via OD was measured as shown in figure 2. It was found that, after being treated by UV-A with and without TiO₂-NPs for 24 hr, the growth of leptospira did not growth as a control growth curve but instead become steady or flat which indicates inactive growth. In contrast, growth curves of both the control and TiO₂-NPs treated groups showed the normal growth behavior which is the exponential growth.

In figure 3, it clearly shows that the number of leptospira when treated by UV-A only or UV-A with TiO_2 -NPs groups for 24 hr of at 7^{th} of cultivation times is less than control and TiO_2 -NPs groups when observed under the DFM. In addition, each cell seems to be lengthier but less mobile (data not shown). Moreover, with a rough estimation, the mobility of the bacteria of both UV-A treated groups is clearly less than 1 μ m/s. However, it should be noted that due to particle aggregation phenomena, causes some of the NPs to form larger particle clusters (about micro-scale

clusters) that have sizes more or less comparable to the sizes of bacteria culture.

In other words, on the basis of growth and motility, leptospira were abnormally immobile when treated by UV-A with and without TiO₂-NPs for 24 hr and exhibited abnormal constant growth when being subcultured. This indicates that most bacteria in UV-A treated groups were mostly dead that explained why they did not reproduce and recover the normal growth when being subcultured and cultivated.

Overall, the data suggests that the control and TiO₂-NPs treated groups have similar features for these studied doses which were not affected significantly from treatment, while both UV-A treatment and UV-A with TiO₂-NPs condition respond similar results. The results indicate that the treatments induce inactivation or death of leptospira in both the short and long term.

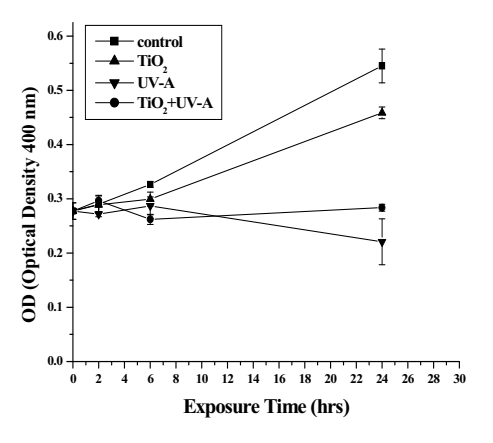


Figure 1: The optical density (OD) of serovar Canicola after being treated with variable time duration. Measurements were done at 400 nm. The key finding is that the data show the similar results when exposed to TiO₂-NPs with and without UV-A irradiation.

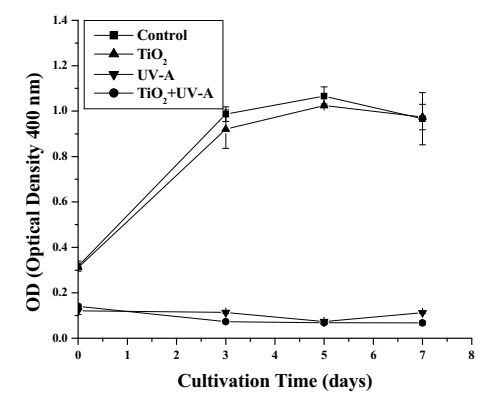


Figure 2: The optical density (OD) of serovar Canicola after being treated for 24 hrs, and subcultured and cultivated in the dark for 7 days. The growths of leptospires did not recover when exposed to UV-A with and without TiO₂-NPs.

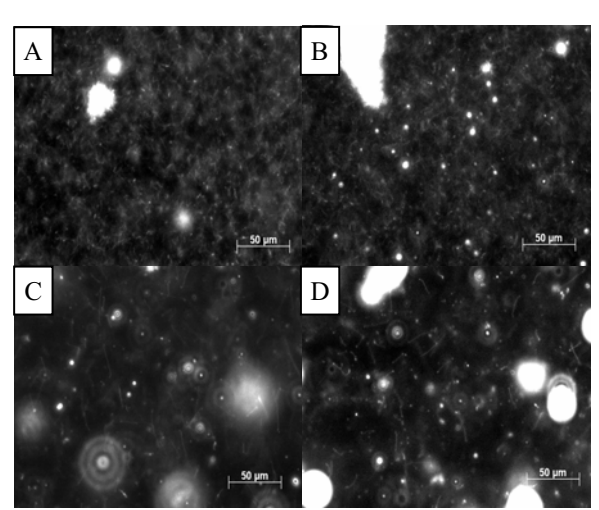


Figure 3: Dark-field optical micrograph (DFM) of serovar canicola at the 7^{th} day of each experimental culture sample. A: is a control unexposed sample, B: is an exposed to TiO_2 -NPs only, C and D: were exposed to UV-A with and without TiO_2 -NPs for 24 hr, respectively. (the scale bar = $50\mu m$)

3.2 Effect on Morphology

At 7th of cultivation times, the leptospira were taken by transmission electron microscopy. In figure 4, it is observed that the leptospira from with and without TiO₂-NPs treated group appeared to be unusual in shape, namely lengthier with longer wavelength and the amplitude or the diameter is clearly thinner (data not shown). We found that the most noticeable of the outer membranes disappears due to UV-A and UV-A with TiO₂-NPs groups and the periplasmic flagella

denature. The periplasmic flagella involved in *Leptospira* motility. This result confirms the DFM images (figure 3) that the leptospira less mobile.

4. DISCUSSION

The objective of these studies was to determine whether TiO₂-NPs has effects on pathogenic *Leptospira interrogans* serovar Canicola with and without UV-A irradiation conditions. The data shows surprisingly similar results for both serovars when treated with UV-A alone and UV-A with TiO₂-NPs. However, the overall nature and direction of the response of spirochetes to UV-A alone is consistent with those we have reported previously for UV-A effects on leptospira [28].

The results of UV-A exposure shown in figure 1 indicate decreases in OD as the exposure or illumination time of UV-A is increased. It is well known that UV-A can induce cellular and molecular changes such as damage to DNA, protein, and lipids in human and bacterial cells [29,30]. UV-A irradiation can induce the formation of reactive oxygen species (ROS) in the cells. These free radicals may cause photoxidation of membrane-bound content and damage the cell membrane. This may result in the lowering of growth and associated denaturation of morphology. However, in the previous findings, there are only data for UV-A effects on other microorganisms especially E. coli. To the best of our knowledge, there is no data that use pathogenic spirochetes as a case study for this similar experimental setup. Therefore, our explanation may be correct if any other unknown subtlety, due to its

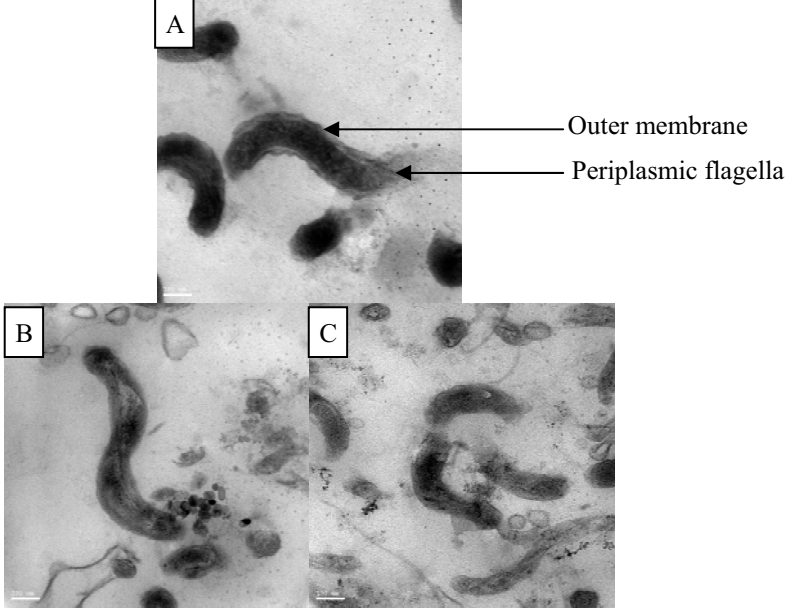


Figure 4: Transmission of electron micrograph of Canicola. Control sample unexposed (A) and exposed to UV-A with (B) and without (C) TiO_2 -NP for 24 hr. (the scale bar = 100nm.)

unique characteristics, plays a crucial role. Briefly, *Leptospira* are spirochete bacteria, which shares characteristics of both Gram-positive and Gramnegative bacteria [13]. As in Gram-positive bacteria,the cytoplasmic membrane of leptospires is closely associated with the peptidoglycan cell wall. The periplasmic flagella reside within the periplasmic space, which provides a barrier shielding underlying antigens and did not readily access the ambient environment [31] while gram-negative bacteria have flagella outside the cell body such as *E. coli*. Grampositive bacteria have an outer membrane, with 2 layers, peptidoglycan and cytoplasmic membranes.

Considering the results of TiO₂-NPs with UV-A irradiation, they surprisingly show the same results of the photocatlytic effect (by UV-A with TiO₂-NPs) and the photolytic effect (by UV-A alone). This is unexpected as far as the previous results (on other types of micro-organisms) concerned [1, 2, 12, 17, 25-We believe that most researchers who are familiar with this subject may expect that using a combination of UV-A and TiO2-NPs will increase the efficacy of damage or bactericidal effects when compared with using UV-A alone. The bactericidal effect of photocatalysis with TiO2-NPs is well recognized, although its mode of action is still poorly characterized. It is believed that radicals or reactive agents produced by TiO2 upon illumination constitute the primary killing agent. The production of extremely reactive hydroxyl radicals by TiO2 photocatalysis combine to give membrane alteration via adsorption, which explains the high efficiency of this disinfection procedure. The bacterial adsorption rate on TiO₂ upon illumination is tightly linked to loss of E. coli viability. In keeping with the importance of adsorption, it is known that hydroxyl radicals formed on the TiO₂ surface display a higher bactericidal efficiency than those free in the solution [10].

The question to be asked now is why the results from figure 1 indicate more or less the same effects due to UV-A without and with TiO2-NPs treatment. These mechanisms are still unclear. Our explanation has a lot to do with the leptospira membrane structure and more importantly mobility of the leptospira. It should be noticed that most or may be all microorganisms used for the similar case studies have much less mobility than leptospira. In fact this is one of the common features of spirochetes. Their cells are very flexible due to the presence of endoflagella and a very thin wall, which results in a characteristic motility which may involve flexing, translocation, screwing, creeping and crawling. In addition, an outer envelope is highly fluid when compared to those of Gram-negative bacteria. This high mobility may decrease the adsorption rate (or cross section) of leptospira to be absorbed on the TiO₂-NPs surface where the interaction between particle and bacterial occurs mostly via ROS. Because of the short half life

of hydroxyl radicals (approximately 10-9 sec) and its low diffusion potential, bacterial targets to be oxidized must be close to the place where they are generated, which in our case is on the TiO₂ particles. Unlike the superoxide, which can be detoxified by superoxide dismutase, the hydroxyl radical cannot be eliminated by an enzymatic reaction, as this would require its diffusion to the enzyme's active site. As diffusion is slower than the half-life of the molecule, it will react with any oxidizable compound in its vicinity. It can damage virtually all types of macromolecules: carbohydrates, nucleic acids (mutations), lipids (lipid peroxidation) and amino acids (e.g. conversion of Phe to m-Tyr and o-Tyr). The only means to protect important cellular structures is the use of antioxidants such as glutathione and of effective repair systems. This hypothesis implies adsorption of bacteria onto TiO₂, which surprisingly has never been reported in the literature before until Gogniat and coworker [32] showed for the first time that adsorption of bacteria on TiO₂ aggregates, and is essential for the bactericidal effect of photocatalysis. They also indicated that bacterial adsorption is influenced by two parameters, composition of the solution used photocatalysis, and duration of illumination. They concluded that interaction between TiO2 and adsorbed bacteria modifies the membrane permeability in the absence of illumination, without directly causing cell death. From the TEM micrographs, we show some abnormalities in shape and outer membrane structure. This seems to be consistent with the previous reports. From figures 2 and 3, the findings confirm that the cells are permanently inactive or dead (by photokilling and photocatalytic killing effects) as can be seen from the 1st subcultured generations of both UV-A and UV-A with TiO₂-NPs treatment which show no growth at all. Indeed, though our findings might not as expected, they are consistent with those of Herrera-Melian and coworker [33]. Their results are similar to ours in such a way that they found little difference between TiO₂ photocatalysis and direct UV-A light irradiation of urban waste waters on total coliforms and Streptoccocus faecalis. Similarly, Robertson et al. [34] found that exposure of all three pathogens (E. coli, Salmonella enterica and Pseudomonas aeruginosa) to UV-A light alone also resulted in a significant reduction in bacterial numbers.

Regarding the mobility, from a biophysical view point, leptospira can swim in highly viscous, gel-like media, such as those containing methylcellulose, that slow down or stop most externally flagellated bacteria [35]. Therefore, in our media, being mixed with TiO₂-NPs, leptospires are still able to swim to protect themselves from ROS or "to hide" themselves in the "TiO₂-NPs shadow" resulting in a decrease of the photocatalytic efficacy. Hence, for UV-A with TiO₂-NPs treatment, the net effects are the combination of both photocatytic effects (with some lost due to the

decrease in the adsorption rate) and compensated photolytic effect. This may be why the net effect from UV-A is comparable to the effect from UV-A with TiO₂-NPs. It should be pointed out that there are limitations to this study. For example, our TiO₂-NPs were bought and in principle will aggregate resulting in the change of the size distribution. In addition, this distribution may depend on several factors such as media type, autoclave, sonicator, illumination time, or doses etc., Therefore, the findings of these studies may not be representative of exposure to commercially specified TiO₂-NPs.

It may be summarized that the UV-A play a major role on antimicrobial effects while the TiO2-NPs affect bacteria only when photocatalysis occurred. Further studies with NPs must be carried out using different doses and/or exposure periods if we want to reach a better understanding. To the best of our knowledge, no published studies have reported on the bactericidal properties of TiO2 on pathogenic spirochetes. This would be an important area of research, especially as it relates to infectious disease prevention. However, the present study is only the first step in assessing the effects of manufactured nanomaterials on deadly pathogenic spirochetes which should be further investigated. From environmental or eco-toxicity aspect, this work may stimulate the fact that release of NPs into the environment could have detrimental effects on biological systems and health.

ACKNOWLEDGEMENTS

We would like to thank Suchada Geawdouanglek, Pranom Puchadapirom and Suraphol Kongtim for technical assistance and helpful discussion, Dr. Toemsak Srikirin for providing UV-A detector, Center of Nano-imaging for the SEM and TEM images and members in Biophysics group (Harit Pitakjakpipop, Titiwat Sungkaworn). This work was supported by The Development and Promotion of Science and Technology Talents Project (DPST), The Thailand Research Fund, The Third World Academy of Sciences (TWAS), and Mahidol University.

REFERENCES

- [1] C. Wei, et al. Environ. Sci. Technol. 28 (1994) 934.
- [2] R.J. Watts, et al. Water. Res. 29 (1995) 95.
- [3] S. Lee, et al. J. Environ. Sci. Health. A. 33 (1998) 1643.
- [4] H. Sakai, et al. BBA-Gen. Subj. 1201 (1994) 259.
- [5] D.M. Blake, et al. Sep. Purif. Meth.28 (1) (1999)1.
- [6] A.V. Emeline, et al. J. Phys. Chem. B. 107 (2003) 7109.
- [7] N. Serpone, The Kirk-Othmer Encyclopedia of Chemical Technology (Wiley, New York, 1996).
- [8] C. Srinivasan and N. Somasundaram, Current. Sci. 85 (2003) 1431.
- [9] J.C. Ireland, et al. Appl. Environ. Microbiol. 59 (1993) 1668
- [10] M. Cho, et al. Appl. Environ. Microbiol. 71 (2005) 270.
- [11] D. Gumy, et al. Appl. Catal. B-Environ. 63 (2006) 76.

- [12] A.G. Rincón, et al. J. Photoch. Photobio. A:Chem. 139 (2001) 233.
- [13] D. Haake, Microbiology. 146 (2000) 1491.
- [14] S.C. Holt, Microbiol. Rev. 42 (1978) 114.
- [15] S. Faine, Guideline for control of leptospirosis, WHO Offset Publ, 67 (1982) 129.
- [16] S. Faine, et al. Leptospira and Leptospirosis 2ed. (Melbourne, Victoria, Australia: MediSci, 1999)
- [17] J.C. Sherris, An introduction to infectious disease (Elsevier, New York, 1990).
- [18] H.C. Ellinghausen and W.G. McCollough, Am. J. Vet. Res. 26 (1965) 45.
- [19] V.F. Stone and R.J. Davis, Chem. Mater. 10 (1998) 1468.
- [20] A.P.T. Kameni, et al. J. Bacteriol. 184 (2002)452.
- [21] H-H. Perkampus, UV-VIS spectroscopy and its application. (New York: Springer-Verlag Berlin Heidelberg,
- [22] S.F. Goldstein and N.W. Charon, Proc. Natl. Acad. Sci. USA. .87 (1990) 4895.
- [23] J.C. Thompson and B.W. Manktelow, J. Comp. Pathol. 96 (1986) 529.
- [24] Z. Huang, et al. J. Photochem. Photobiol. A: Chem. 130 (2000) 163.
- [25] H-L. Liu, et al. Process. Biochem. 39 (2003) 475.
- [26] O. Seven, et al. J. Photochem. Photobiol. A: Chem. 165 (2004) 103.
- [27] J.A. Ibáñez, et al. J. Photochem. Photobiol:C. 157 (2003) 81.
- [28] J. Wong-ekkabut, et al. In press.
- [29] J. Cadet, et al. Mutat. Res-Fund. Mol. M. 571 (2005) 3.
- [30] G.P.Pfeifer, et al. Mutat. Res-Fund. Mol. M. 571 (2005) 19.
- [31] J.L. Coleman and J.L. Benach, J. Clin. Invest. 84 (1989) 322.
- [32] G. Gogniat, et al. FEMS Microbiol. Lett. 258 (2006)18.
- [33] J.A.H. Melian, et al. Chemosphere. 41 (2000) 323.
- [34] J.M.C. Robertson, et al. J. Photochem. Photobiol. A:Chem. 175 (2005) 51.
- [35] N.W. Charon and S.F. Goldstein, Annu. Rev. Genet. 36 (2002) 47.